A 19-Month Record of Marine Aerosol–Cloud–Radiation Properties Derived from DOE ARM Mobile Facility Deployment at the Azores. Part I: Cloud Fraction and Single-Layered MBL Cloud Properties

XIQUAN DONG, BAIKE XI, AND AARON KENNEDY

Department of Atmospheric Sciences, University of North Dakota, Grand Forks, North Dakota

PATRICK MINNIS

Science Directorate, NASA Langley Research Center, Hampton, Virginia

ROBERT WOOD

Department of Atmospheric Sciences, University of Washington, Seattle, Washington

(Manuscript received 11 September 2013, in final form 18 December 2013)

ABSTRACT

A 19-month record of total and single-layered low (<3 km), middle (3–6 km), and high (>6 km) cloud fractions (CFs) and the single-layered marine boundary layer (MBL) cloud macrophysical and microphysical properties was generated from ground-based measurements at the Atmospheric Radiation Measurement Program (ARM) Azores site between June 2009 and December 2010. This is the most comprehensive dataset of marine cloud fraction and MBL cloud properties. The annual means of total CF and single-layered low, middle, and high CFs derived from ARM radar and lidar observations are 0.702, 0.271, 0.01, and 0.106, respectively. Greater total and single-layered high (>6 km) CFs occurred during the winter, whereas single-layered low (<3 km) CFs were more prominent during summer. Diurnal cycles for both total and low CFs were stronger during summer than during winter. The CFs are bimodally distributed in the vertical with a lower peak at ~1 km and a higher peak between 8 and 11 km during all seasons, except summer when only the low peak occurs. Persistent high pressure and dry conditions produce more single-layered MBL clouds and fewer total clouds during summer, whereas the low pressure and moist air masses during winter generate more total and multilayered clouds, and deep frontal clouds associated with midlatitude cyclones.

The seasonal variations of cloud heights and thickness are also associated with the seasonal synoptic patterns. The MBL cloud layer is low, warm, and thin with large liquid water path (LWP) and liquid water content (LWC) during summer, whereas during winter it is higher, colder, and thicker with reduced LWP and LWC. The cloud LWP and LWC values are greater at night than during daytime. The monthly mean daytime cloud droplet effective radius r_e values are nearly constant, while the daytime droplet number concentration N_d basically follows the LWC variation. There is a strong correlation between cloud condensation nuclei (CCN) concentration N_{CCN} and N_d during January–May, probably due to the frequent low pressure systems because upward motion brings more surface CCN to cloud base (well-mixed boundary layer). During summer and autumn, the correlation between N_d and N_{CCN} is not as strong as that during January–May because downward motion from high pressure systems is predominant. Compared to the compiled aircraft in situ measurements during the Atlantic Stratocumulus Transition Experiment (ASTEX), the cloud microphysical retrievals in this study agree well with historical aircraft data. Different air mass sources over the ARM Azores site have significant impacts on the cloud microphysical properties and surface CCN as demonstrated by great variability in N_{CCN} and cloud microphysical properties during some months.

1. Introduction

Owing to their substantial role in the earth's radiation budget, and consequently their effect on the earth's climate, low-level stratiform clouds have been a topic of

Corresponding author address: Dr. Xiquan Dong, Department of Atmospheric Sciences, University of North Dakota, 4149 Campus Road, Box 9006, Grand Forks, ND 58202-9006.
E-mail: dong@aero.und.edu

DOI: 10.1175/JCLI-D-13-00553.1

© 2014 American Meteorological Society

considerable interest since publication of the classic paper describing their physics (Lilly 1968). Low-level stratiform clouds are often defined, from the satellite perspective, as clouds with tops beneath 680 hPa (~3.3 km) and include stratus, stratocumulus, and shallow cumulus (Rossow and Schiffer 1991). These low-level clouds can form within both deep and shallow marine boundary layers (MBLs) (defined as cloud-top heights lower than 3 km in this study). MBL clouds in the subtropical regions strongly influence the regional and global climate system (e.g., Klein and Hartmann 1993). The most extensive MBL clouds occur over the east side of subtropical oceans, and over midlatitude oceans under conditions of modest cold air advection during periods of equatorward flow (Klein and Hartmann 1993). A strong temperature inversion at the top of the MBL, which is maintained by large-scale subsidence combined with cold sea surface temperatures, provides conditions favorable for MBL cloud formation (Lilly 1968). These MBL clouds are maintained by vertical mixing primarily due to the strong longwave radiative cooling at the cloud top because the radiative cooling generates turbulence to maintain an upward moisture flux (Albrecht et al. 1995; Paluch and Lenschow 1991; Rémillard et al. 2012).

MBL clouds and their interactions with aerosols are extremely important components of the climate system (Wood 2012). Their treatment in climate models is one of the largest sources of uncertainty in predicting any potential future climate change (Wielicki et al. 1995; Houghton et al. 2001; Bony and Dufresne 2005). Although many improvements have been made in phase 5 of the Coupled Model Intercomparison Project (CMIP5) (Taylor et al. 2012; Klein et al. 2013; Jiang et al. 2012), MBL clouds are still a problem in climate models (e.g., Stanfield et al. 2014; Dolinar et al. 2014) and numerical weather prediction (NWP) models such as theNOAA Global Forecasting System (GFS) (Yoo and Li 2012; Yoo et al. 2013). Because their structural and optical properties are strongly dependent upon interactions between aerosol/cloud microphysics and dynamics, these intricate interactions involve the formation of precipitation and its effect upon cloud dynamics, turbulence, and entrainment (Wood 2012). However, there continues to be a lack of understanding of many key physical links between aerosol and cloud microphysical properties. In addition, we do not have sufficient observations to accurately quantify the multivariate sensitivity of precipitation to cloud microphysical and macrophysical properties. Therefore, such studies are essential for the evaluation of both climate and process-based numerical models.

The climatic importance of the microphysical and macrophysical properties of MBL clouds, particularly the cloud fraction, cloud-droplet effective radius (r_e), number concentration (N_d), and liquid water content (LWC) and liquid water path (LWP), is widely recognized. Early studies found that the albedo effect of these clouds is important and leads to a strong net cooling of the Earth System (Hartmann and Short 1980). Slingo (1990) used a climate model to show that a modest relative increase of 15%–20% in the cloud fraction coupled with a 15%–20% decrease in r_e and a 20%–30% increase in LWP could balance the radiative perturbation associated with doubled CO_2 concentrations. Cess et al. (1990) compared 19 GCMs and found a variety of cloud feedback results, ranging from modestly negative to strongly positive, because various climate models have different representations of cloud microphysical and radiative properties. An updated comparison by Cess et al. (1996) showed a narrowed difference with most models producing modest cloud feedback. This was a result of corrections to cloud optical properties in the models such as improved r_e values. Recent studies, however, indicate little narrowing in the cloud feedback spread of the latest model versions (Soden and Vecchi 2011; Dolinar et al. 2014). It is therefore imperative to have more accurate MBL cloud microphysical properties through long-term ground-based observations so that we can improve their representation in climate models.

The Department of Energy (DOE) Atmospheric Radiation Measurement (ARM) Mobile Facility (AMF) was deployed on the northern coast of Graciosa Island, Azores (39.09°N, 28.03°W), for approximately 19 months (June 2009–December 2010) to study the seasonal and diurnal variations of MBL clouds and to increase understanding of their formation and dissipation processes over the remote subtropical northeast Atlantic Ocean (NEA) (Wood 2009; Wood et al. 2014). Long-term comprehensive ground-based observations at Graciosa Island make up an invaluable data source for investigating seasonal and diurnal variations of MBL cloud fraction and macrophysical and microphysical properties, as well as their interactions with aerosols and large-scale synoptic patterns. These AMF#1 (henceforth AMF) ground-based observations have renewed the ground-based observations over the NEA of the 1992 Atlantic Stratocumulus Transition Experiment (ASTEX) (Albrecht et al. 1995), which provided a monthlong record and was one of the first successful deployments of millimeter radars for studying MBL clouds.

As the first part of a series, this paper documents fundamental statistical information about seasonal and diurnal variations of 1) total and single-layered low (<3 km), middle, and high (>6 km) cloud fractions and their vertical distributions and 2) single-layered daytime MBL cloud (cloud-top heights <3 km, including stratus,

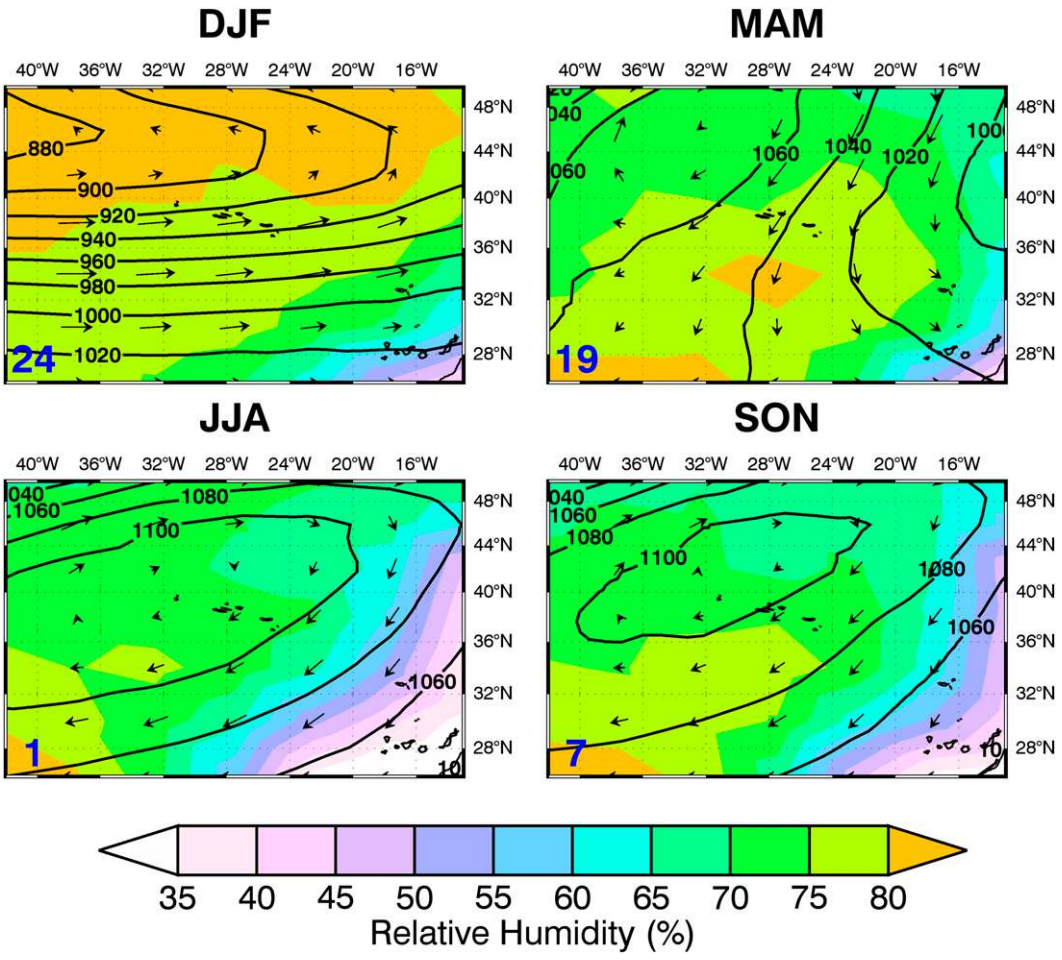

FIG. 1. 900-hPa analysis based on the National Aeronautics and Space Administration Modern-Era Retrospective Analysis for Research and Applications (MERRA) reanalysis during the period June 2009–December 2010. The grid box covers a range of latitudes from 26° to 50°N and longitudes from 42° to 12°W centered on the ARM Azores site. Shown are 900-hPa geopotential heights, wind vectors, and shaded contours of relative humidity. The four seasons are winter (DJF), spring (MAM), summer (JJA), and fall (SON).

stratocumulus, and shallow cumulus) macrophysical and microphysical properties over the Azores during June 2009–December 2010. The present work, which uses 19 months of nearly continuous ground-based cloud observations, should provide the most comprehensive and reliable estimates of seasonal and diurnal variations of marine cloud fraction, MBL cloud macro- and microphysical properties, and influences of large-scale dynamics. The results will provide a valuable dataset for advancing the understanding of MBL cloud processes and properties and enabling climate/forecast modelers to more fully evaluate simulations over the NEA.

2. Datasets and large-scale synoptic patterns

Graciosa Island is an ideal location to study marine boundary layer (MBL) clouds because it is sufficiently remote to be clear of direct continental influence (1300 km from Europe). Also, island effects on measurements are minimal because winds are predominantly from the north and west as shown in Fig. 1. The Azores typically experience relatively clean conditions advected from the central North Atlantic that produce nearly pristine MBL clouds, but periodically experience episodes of polluted air masses advected from western Europe, North Africa, and North America (see Fig. 1 of Logan et al. 2014; Wood et al. 2013, manuscript submitted to *Bull. Amer. Meteor. Soc.*) that enrich the MBL clouds with aerosols (Albrecht et al. 1995; Dong et al. 1997; Wood 2009; Wood et al. 2013, manuscript submitted to *Bull. Amer. Meteor. Soc.*; Logan et al. 2014). The NEA is a region of persistent but diverse subtropical MBL clouds. As illustrated in Fig. 1, subsidence from a persistent high pressure system over the Azores during the summer months gives rise to

TABLE 1. Cloud property measurement and retrieval methods used at AMF (Azores).

Cloud parameter	Instruments/methods	Uncertainty	References
Cloud-base height	Ceilometer	15 m	Rémillard et al. (2012)
Cloud-base height	Micropulse lidar	30 m	Clothiaux et al. (2000)
Cloud-top height	Microwave cloud radar	43 m	Rémillard et al. (2012)
Cloud-base and -top temperatures	Merged sounding	0.2°C	ARM website (www.arm.gov)
Cloud LWP	Microwave radiometer	~20 g m^{-2} for LWP < 200 ~ 10% for LWP > 200	Dong et al. (2000); Liljegren et al. 2001
Cloud LWC	LWP/cloud thickness		
r_e	Parameterization $r_e = 2.07 + 2.49\text{LWP} + 10.25\gamma - 0.25\mu_0 + 20.28\text{LWP}\gamma - 3.14\text{LWP}^*\mu_0$	~10% for daytime	Dong et al. (1997, 1998, 2002)
N_d	Parameterization $N_d = \text{LWC}/[(4/3)\pi\rho_w r_e^3 \exp(-3\sigma_X^2)]$	~20%–30% for daytime	Dong et al. (1997, 1998, 2002)
τ	Parameterization $\tau = 1.5\text{LWP}/r_e$	~10% for daytime	Dong et al. (1997, 1998, 2002)
CCN	AMF Aerosol Observing System	~	ARM web page (www.arm.gov); Jefferson (2010); Wood et al. (2013, manuscript submitted to *Bull. Amer. Meteor. Soc.*); Hudson and Noble (2014)
γ	SW↓(cloud)/SW↓(clear)	~5% for daytime	Long and Shi (2008)

relatively dry conditions [relative humidity (RH) ~65%–75%] and a transition from an overcast stratocumulus regime to a broken trade cumulus regime. In contrast, low pressure systems tend to be located north-northwest of the Azores during the winter months, which induce anomalous westerly winds that transport moist air masses (RH ~75%–85%) from the North Atlantic to the Azores, producing more multilayered clouds and deep frontal clouds associated with mid-latitude cyclones.

Cloud macrophysical properties such as fraction, height, thickness, and temperature are taken directly from the AMF merged soundings, radar, ceilometer, and lidar measurements. Primary AMF cloud observations and retrievals, and their uncertainties and references, are listed in Table 1. The centerpiece of the cloud instrument array is the 95 GHz W-band ARM Cloud Radar (WACR) (Mead and Widener 2005). The WACR operates at a wavelength of 3.15 mm in a vertically pointing mode (beamwidth 0.19°) and provides continuous profiles (2-s temporal and 43-m vertical resolution) of radar reflectivity from hydrometeors moving through the radar field of view, which allows for the identification of clear and cloudy conditions. The WACR is sensitive enough (−50 dBZ at 2 km) to detect MBL small cloud droplets and large light to moderate drizzle drops (Rémillard et al. 2012).

The cloud fraction (CF) is simply the percentage of radar/lidar returns that are cloudy within a specified sampling time period (e.g., month). It is given by the ratio of the number of hours when both the radar and lidar/ceilometer detected clouds to the total number of hours when all measurements (radar/lidar/ceilometer) were available. This study uses approximately 12 950 h for all-sky samples, which is 94% of all possible data during the 19-month period [for more details about the instruments up/down time, see Fig. 1 of Rémillard et al. (2012)]. The total cloud fraction CF_T is the fraction of time when a cloud is detected anywhere in the vertical column, the single-layered low cloud fraction CF_L is the fraction of time when low clouds ($Z_{\text{top}} < 3$ km) occur without clouds above them, the high cloud amount CF_H is determined for clouds having Z_{base} higher than 6 km with no clouds underneath, while middle clouds (CF_M) range from 3 to 6 km with no clouds either above or below. Although CF_T, CF_L, CF_M, and CF_H are computed using the same denominator (all-sky samples), CF_T does not equal the sum of CF_L, CF_M, and CF_H because CF_T includes all cloudy conditions, such as some deep convective clouds and multilayered clouds that did not satisfy our definitions of single-layered low/middle/high cloud layers. These cloud fractions should not be confused with the instantaneous hemispheric cloud fractions observed by satellite and surface observations (Dong et al. 2005).

Cloud-top height (Z_{top}) is derived from cloud radar reflectivity profiles while cloud-base height (Z_{base}) is derived from a composite of Vaisala laser ceilometer, micropulse lidar (MPL), and cloud radar data (Clothiaux et al. 2000; Mather and Voyles 2013). Cloud-base and -top temperatures, T_{base} and T_{top} respectively, are estimated from ARM merged soundings (interpolated rawinsonde

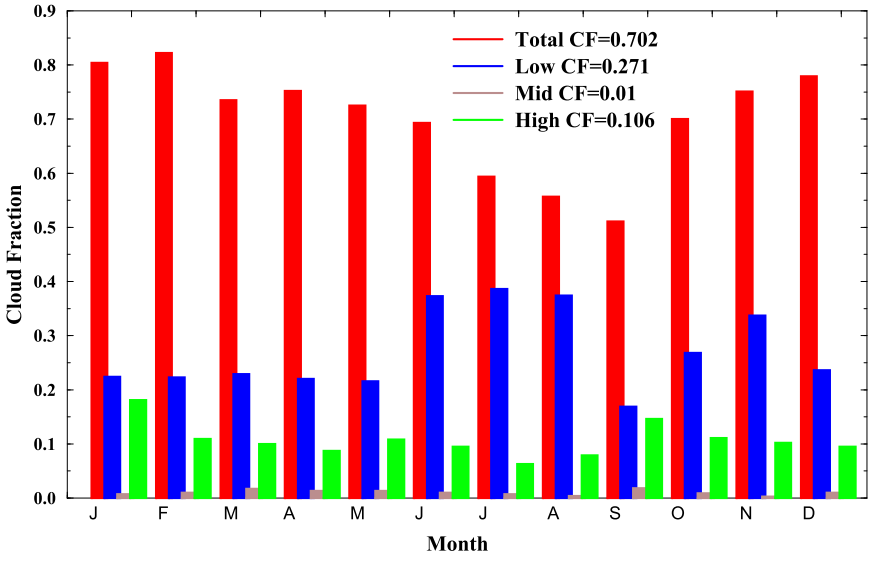

FIG. 2. Monthly mean cloud fractions derived from DOE ARM radar/lidar measurements during the DOE ARM Mobile Facility (AMF) June 2009–December 2010 deployment at Graciosa Island, Azores (39.09°N, 28.03°W). Total CF includes any clouds above the radar/lidar instruments. Single-layered clouds: low CF ($Z_t \le 3$ km), mid CF ($Z_b > 3$ km, $Z_t \le 6$ km), and high CF ($Z_t > 6$ km).

soundings with other measurements and corrections, such as normalization to the total atmospheric column water vapor retrieved from the microwave radiometer data) using Z_{base} and Z_{top}. Cloud physical thickness (ΔZ) is simply the difference between Z_{top} and Z_{base}. The LWP is derived from the microwave radiometer brightness temperatures measured at 23.8 and 31.4 GHz using a statistical retrieval method (Liljegren et al. 2001). The AMF up- and down-looking standard Eppley Precision Spectral Pyranometers (PSPs) provide measurements of downwelling and upwelling broadband shortwave (SW) (from 0.3 to 3 μm) fluxes with uncertainties of roughly 10 W m^{-2} (Long and Shi 2008).

The daytime microphysical and radiative properties of single-layered MBL clouds are retrieved from the SW and LWP data. A δ2-stream radiative transfer model is used to compute the downwelling SW flux. The retrieval scheme of Dong et al. (1997) is based on an iterative approach that varies cloud-droplet effective radius (r_e) and number concentration (N_d) in the radiative transfer calculations until the model-calculated solar transmission matches the measured one. Dong et al. (1998) parameterized the retrieved r_e as a function of LWP, the solar transmission, and cosine of the solar zenith angle (μ_0). The optical depths are derived from the ratio of LWP to r_e. The retrieved and parameterized low-cloud microphysical properties have been validated by in situ aircraft measurements at midlatitude continental sites (Dong et al. 1998, 2002; Dong and Mace 2003). The cloud condensation nuclei (CCN) concentration (N_{CCN}) was calculated using measurements from an optical particle counter at 0.2% supersaturation by the AMF Aerosol Observation System at the Azores site (Jefferson 2010; Wood et al. 2013, manuscript submitted to *Bull. Amer. Meteor. Soc.*). Notice that N_{CCN} increases with increasing supersaturation (Hudson and Noble 2014; Wood et al. 2013, manuscript submitted to *Bull. Amer. Meteor. Soc.*), while N_{CCN} at 0.2% supersaturation can represent the mean atmospheric condition. Although both daytime and night N_{CCN} results are available, we only use the daytime N_{CCN} to maintain consistency with the daytime MBL cloud microphysical retrievals in this study.

To help ensure reliable daytime cloud microphysical retrievals, the cloudy cases selected in this study are single-layered and overcast low clouds that persist for approximately 2 h over the AMF site. The MBL clouds primarily include stratus and stratocumulus in addition to some shallow cumulus clouds with cloud-top heights less than 3 km. Five criteria were established for choosing the conditions under which daytime cloud properties can be estimated: (i) only single-layer and overcast low clouds are present as determined from cloud radar/lidar observations, (ii) $Z_{\text{top}} < 3$ km, (iii) $20 <$ LWP < 700 g m^{-2}, (iv) $\mu_0 > 0.1$, and (v) $0.08 <$ solar transmission (γ) < 0.7. The physical reasons for these five criteria are discussed by Dong et al. (2000). Approximately 1091 h (~13 092 samples at 5-min resolution) of daytime data satisfied the above criteria during the 19-month period.

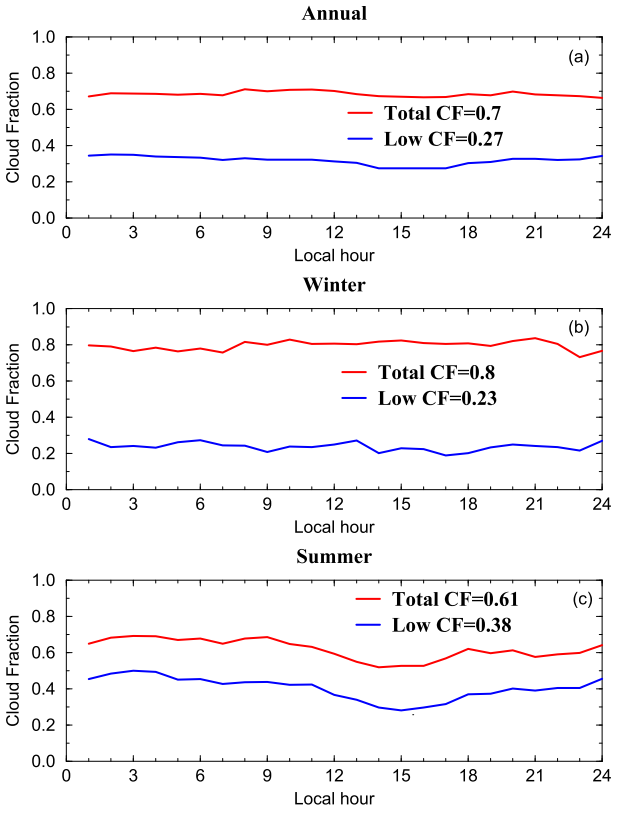

FIG. 3. As in Fig. 2, but for hourly mean cloud fraction derived from ARM radar/lidar observations at the ARM Azores site during the 19-month period. Local hour at the ARM Azores site is UTC − 1 h. The means for annual, winter, and summer data are shown at each panel for total and low cloud fractions, respectively.

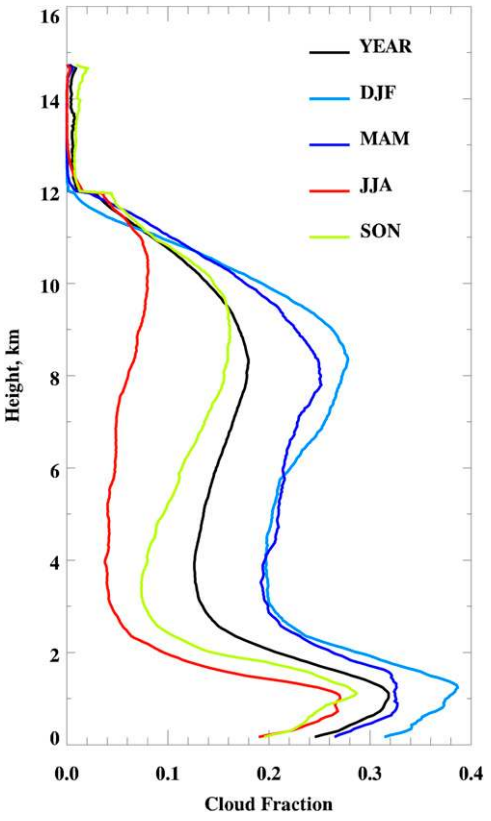

FIG. 4. Mean vertical distributions of CF derived from the ARM radar/lidar observations with a vertical resolution of 43 m and a temporal resolution of 5 min at the ARM Azores site, June 2009–December 2010.

3. Cloud fraction

In this section, seasonal and diurnal variations of total and single-layered CFs, as well as their vertical distributions, are presented in Figs. 2–4. The 10 CF categories at the ARM Azores site during the 19-month period are summarized in Table 2. Finally we discuss the similarities and differences between this study and Rémillard et al. (2012). Four seasons are defined as winter [December–February (DJF)], spring [March–May (MAM)], summer [June–August (JJA)], and autumn [September–November (SON)] in this study.

a. Seasonal variation

Monthly variations of total cloud fraction (CF_T) and single-layered low (CF_L), middle (CF_M), and high (CF_H) cloud fractions during the 19-month period are illustrated in Fig. 2 and summarized in Table 2. Monthly means of CF_T decrease from winter to summer, reach a minimum during September, and then gradually increase from September to December with an annual average of 0.702. CF_L values remain nearly constant (0.22) from January to May, followed by a significant increase to 0.38 during June–August, and then fluctuate from 0.17 to 0.34 during September–December. Notice that during summer the majority of clouds are single-layered low clouds (CF_L = 0.38 vs CF_T = 0.61) owing to a persistent high pressure system (Fig. 2) and nearly 100% inversion-topped MBLs (Fig. 5a in Rémillard et al. 2012). Multilayered clouds are the majority cloud type during winter when the sum of all single-layered clouds is nearly 0.37 (vs CF_T = 0.8). The monthly variation of CF_H is almost the same as that of CF_T, decreasing from winter to summer, but mirrors the variation of CF_L. Single-layered middle clouds occur least frequently and are seasonally invariant. Annual means of CF_L, CF_M, and CF_H are 0.271, 0.01, and 0.106, respectively, indicating that both single-layered middle and high clouds occur much less frequently than single-layered low clouds at the Azores during the 19-month period.

b. Diurnal cycle

Figure 3 shows the hourly means of CF_T and CF_L for all of the data and for winter and summer separately. Hourly mean CFs were calculated from all samples in

TABLE 2. Summary of 10 cloud categories at the ARM Azores site (June 2009–December 2010).

Cloud type	Definition (km)	Annual	Winter	Summer
1	Single low, <3 km	0.271	0.228	0.377
2	Single middle, 3–6 km	0.01	0.009	0.007
3	Single high, >6 km	0.106	0.128	0.078
4	Middle over low, contiguous	0.022	0.034	0.009
5	High over middle, contiguous	0.023	0.033	0.007
6	High over both mid and low, contiguous	0.036	0.064	0.007
7	Middle over low, noncontiguous	0.02	0.028	0.011
8	High over middle, noncontiguous	0.025	0.028	0.01
9	High over low, noncontiguous	0.103	0.156	0.032
10	High over mid and low, noncontiguous	0.085	0.089	0.074
Sum	Total CF	0.70	0.80	0.613

that local hour (such as between 0100 and 0200 LT, presented at 0200 LT in Fig. 3) during the 19-month period. For the annual and winter periods, hourly means of their CF_T and CF_L are relatively invariant. During summer, however, there are strong diurnal variations in both CF_T and CF_L where the variation in CF_T basically follows CF_L (Fig. 3c). For example, both CFs remain nearly constant from midnight (0000 LT) to 1000 LT, decrease from 1100 to 1500 LT followed by an increase to 1900 LT, and finally level off for the remainder of the night. The annual, winter, and summer hourly mean CF_T differences (ΔCF_T = Max − Min) are 0.041 (0.041/0.70 = 5.9%), 0.103 (12.9%), and 0.173 (27.6%), respectively. For CF_L differences, they are 0.065 (22.6%), 0.086 (40%), and 0.208 (56.2%), respectively. The CF_L and CF_T maxima occur during night and morning with minima during afternoon. This day − night difference is most pronounced during summer, consistent with the results in Wood (2012, Fig. 8a) although his definition of low cloud amount differs from that in this study. This strong diurnal variation in CF_L results from mixing driven by nocturnal longwave radiative cooling at the cloud top that is not countered by solar absorption at night (Albrecht et al. 1995; Paluch and Lenschow 1991; Wood 2012; Rémillard et al. 2012). During the day, the absorption of solar radiation near the cloud top warms the cloud layer and partially offsets the longwave radiative cooling, which suppresses turbulence and cloud formation within MBL.

c. Vertical distribution

Figure 4 shows the annual and seasonal mean vertical distributions of CF derived from the ARM radar/lidar observations with a 43-m vertical resolution during the 19-month period. During summer, the CF profile is strongly peaked at 1 km with typical CF values of ~0.05 above 2 km. A very minor secondary maximum is seen near 11 km. For the other seasons, and hence for the annual mean, the CF vertical distributions are strongly bimodal, with primary and secondary peaks at roughly 1 km and between 8 and 9 km, respectively. The winter and spring seasons experience not only more middle and high clouds, but also more low clouds than other seasons despite the summertime maximum in single-layered low clouds. The cold season low-cloud maximum is due to increased multilayered clouds. Seasonal synoptic patterns (Fig. 1) provide strong support for the results in Figs. 2–4. That is, persistent high pressure and dry conditions explain more single-layered MBL clouds and fewer total clouds during summer months while the low pressure and moist air masses during winter months result in more occurrences of total and multilayered clouds as well as more deep frontal clouds associated with midlatitude cyclones.

To further investigate CF vertical distributions, the ARM radar/lidar-derived CFs have been classified into 10 categories (see summary in Table 2) that represent different cloud formation and dissipation processes and different large-scale dynamics. The definitions of these 10 categories have been discussed in detail by Xi et al. (2010). Basically, the definitions of single-layered low/middle/high clouds are the same as in Fig. 2. The percentages of categories 1–3 in Table 2 are the same as the results in Fig. 2, while the percentages in both categories 4 and 6 represent cumulus or convective clouds and the percentage in category 5 is for physically thick cirrus clouds. Technically speaking, categories 4–6 belong to single-layered clouds, but they do not fit into the definitions of single-layered low, middle, and high clouds in this study, while categories 7–10 are multilayered clouds. Based on this discussion, the single-layered (sum of categories 1–6) and multilayered (sum of categories 7–10) CFs are 0.468 and 0.233 for the annual mean, 0.496 and 0.305 for winter, and 0.485 and 0.127 for summer. The results in Table 2 reveal the magnitude of the winter − summer difference in multilayered cloud CFs. Table 2 also shows that there are more deep frontal clouds associated with midlatitude cyclones and/or convective clouds during winter than during summer at the Azores (category 6 = 0.064 and 0.007 for winter and summer, respectively).

d. Discussion

Rémillard et al. (2012) provided the operational status of AMF WACR, ceilometer, and MWR, as well as different types of cloud occurrences during the 19-month

TABLE 3. Seasonal and yearly averages, standard deviations, medians, and modes of various cloud parameters derived from the 19-month ARM Azores dataset.

Winter		Spring		Summer		Autumn		Year	
Day	Night	Day	Night	Day	Night	Day	Night	Day	Night
				CF					
0.231	0.215	0.215	0.212	0.352	0.370	0.259	0.284	0.282	0.295
				Z_{base} (km)					
1.14	1.12	1.15	1.08	0.76	0.79	1.0	0.98	0.92	0.95
0.48	0.4	0.51	0.52	0.47	0.47	0.48	0.48	0.51	0.49
1.15	1.12	1.17	1.06	0.73	0.76	0.96	0.92	0.88	0.91
1.5	1.1	1.5	0.7	0.3	0.7	0.09	0.9	0.9	0.9
				Z_{top} (km)					
1.77	1.78	1.75	1.71	1.31	1.35	1.47	1.51	1.46	1.52
0.53	0.47	0.54	0.56	0.50	0.48	0.51	0.51	0.54	0.52
1.82	1.73	1.82	1.69	1.3	1.3	1.43	1.52	1.43	1.52
1.9	1.7	1.9	1.75	1.3	1.3	1.9	1.1	1.3	1.3
				Z (km)					
0.63	0.66	0.6	0.63	0.55	0.56	0.48	0.53	0.55	0.58
0.45	0.4	0.42	0.46	0.43	0.42	0.34	0.36	0.41	0.41
0.49	0.55	0.48	0.49	0.4	0.42	0.37	0.42	0.41	0.45
0.4	0.3	0.3	0.3	0.3	0.3	0.3	0.3	0.3	0.3
				T_{base} (K)					
277.2	276.7	278.3	278.5	287.4	287.3	283.8	283.2	284.3	283.2
4.5	3.8	4.4	4.8	3.9	4.0	4.9	5.2	5.7	6.0
276.4	276.6	277.9	278.5	287.7	287.5	285.0	283.8	285.1	283.8
277.5	277.5	277.5	277.5	287.5	287.5	287.5	287.5	287.5	287.5
				T_{top} (K)					
274.7	274.2	276.2	276.1	286.0	285.8	283.1	282.2	282.9	281.7
4.5	4.7	3.9	4.4	3.5	3.6	4.8	5.2	5.8	6.2
274.6	274.5	276.1	276.4	286.0	286.3	284.1	283.1	284.3	282.8
272.5	277.5	277.5	277.5	287.5	287.5	287.5	287.5	287.5	287.5
				LWP ($g\,m^{-2}$)					
99.0	147.4	121.8	138.4	114.4	148.8	93.3	124.6	108.7	139.6
92.0	144.9	119.9	133.4	96.3	129.6	76.9	115.4	96.0	129.1
65.7	90.6	75.2	87.5	81.4	100.9	68.7	84.5	75.4	91.6
25	25	25	75	75	75	75	75	75	75
				LWC ($g\,m^{-3}$)					
0.16	0.23	0.22	0.24	0.24	0.29	0.21	0.25	0.22	0.26
0.14	0.21	0.18	0.18	0.17	0.26	0.15	0.19	0.17	0.22
0.12	0.17	0.17	0.19	0.2	0.23	0.18	0.2	0.18	0.2
0.05	0.05	0.15	0.16	0.15	0.16	0.15	0.16	0.15	0.16
				r_e (μm)					
12.4		12.6		12.7		12.0		12.5	
5.1		4.6		4.4		4.6		4.6	
11.5		12.0		12.2		11.2		11.9	
9		11		11		11		11	
				N_d (cm^{-3})					
75.4		76.8		82.5		89.1		82.6	
117.7		113.4		137.9		110.8		126.2	
36.3		40.3		43.5		52.4		44.1	
5		15		15		15		15	
				N_{CCN} (cm^{-3})					
265.6		235.3		192.5		196.1		207.3	
222.7		195.9		109.8		114.8		143.8	
173.9		162.7		173.8		180.4		175.0	
125		75		125		175		125	

TABLE 3. (*Continued*)

Winter		Spring		Summer		Autumn		Year	
Day	Night	Day	Night	Day	Night	Day	Night	Day	Night
				τ					
12.1		14.9		14.0		12.1		13.5	
8.4		12.7		9.7		7.3		9.6	
10.0		10.9		11.4		10.5		11.0	
7.5		7.5		7.5		7.5		7.5	

period at the Azores. They primarily focused on MBL clouds and investigated their cloud structural and dynamical properties, such as cumulus and stratocumulus cloud fractions and associated LWP, drizzle, and precipitation. In this study, we provide the statistical results of total and single-layered low, middle, and high cloud fractions, as well as their vertical distributions, but do not provide different MBL cloud types and drizzle/precipitation. There are some similarities and differences between these two studies. For example, their low clouds were defined as cloud-top heights lower than 3 km (similar to this study), but their middle and high clouds were defined as cloud-base heights above 3 and 7 km, respectively (Table 2 in Rémillard et al. 2012). Also their low, middle, and high cloud occurrences (Fig. 3b in Rémillard et al. 2012) represented all cloudy conditions (both single layer and multilayer), while the monthly mean CFs in Fig. 2 are representative of single-layered low, middle, and high clouds. Nevertheless, their total cloud occurrence (Fig. 3a in Rémillard et al. 2012) was nearly identical to the CF_T in Fig. 2, confirming that both studies used the same datasets and had the same total cloud fraction during the 19-month period. Although there are some overlaps between these two studies, they complement each other. Therefore the combination of these two studies will provide a more complete characterization of the marine clouds and MBL clouds at the Azores.

4. Single-layered low cloud properties

In this section, all cloud properties are derived from single-layered low clouds with cloud-top heights below 3 km and no overlying clouds. Note that in this study, these clouds are defined as MBL clouds although they can form within both deep and shallow MBLs, which differs slightly from the traditional definition. In particular, the monthly mean daytime MBL cloud macrophysical properties, such as cloud-base and -top heights and temperatures and thickness, are presented in Fig. 5, and daytime microphysical properties are presented in Fig. 7. Their corresponding daytime (and night) frequency distribution functions (PDFs) and cumulative distribution functions (CDFs) are illustrated in Figs. 6 and 8, respectively. Their seasonal and yearly mean, standard deviation, median, and mode values are listed in Table 3. Diurnal variations of MBL cloud macrophysical and microphysical properties are shown in Fig. 9.

a. *Macrophysical properties*

Monthly mean daytime MBL cloud macrophysical properties derived from the 19-month Azores dataset along with variations about the means are represented as box-and-whisker plots in Fig. 5. In each plot, the bottom and top of each whisker represent the 5th and 95th percentiles of the PDFs, the bottom and top of each box represent 25th and 75th percentiles of the PDF, and the shorter and longer lines across each box represent the median and mean, respectively. The distribution at the far right (ANN) of each plot shows the cumulative statistics from the entire daytime dataset during the 19-month period. The average for the dataset is given by the horizontal line extending across the entire plot. Monthly mean cloud-base and -top heights (Figs. 5a and 5b) are above their annual means (Z_{base} = 1.016 km, Z_{top} = 1.575 km) from December through May followed by a significant decrease in June, and then remain below or close to their annual means until November. Cloud thickness ($\Delta Z = Z_{top} - Z_{base}$) in Fig. 5c basically follows the cloud layer variation. That is, the cloud depth, on average, is about 100 m thicker during winter and spring than during summer and autumn. These results are also consistent with those in Fig. 4 where the primary frequency maxima during winter and spring occur at slightly higher altitudes than those during summer and autumn. Annual mean cloud-base (T_{base}) and -top temperatures (T_{top}) are 281.8 and 280.1 K, respectively. Monthly T_{base} and T_{top} averages basically follow the seasonal variation of surface temperature and mirror their height variations, such as being below their annual means from December to May but being above the means from June to November. These results indicate that the MBL cloud layer, depth, and temperature are deeper, thicker, and cooler, respectively, from December to May than from June to November in this study. This result is consistent with estimates of the seasonal variation of low clouds off the Californian coast (Lin et al. 2009).

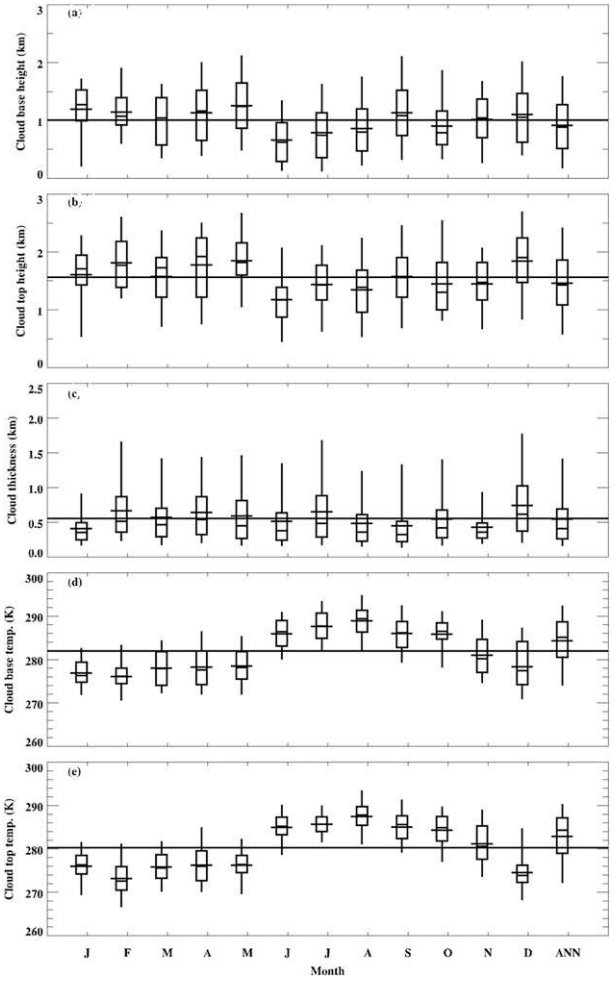

FIG. 5. Monthly mean daytime single-layered marine boundary layer (MBL) cloud macrophysical properties derived from a total of 19 months ARM Azores observations. The bottom and top of each whisker represent the 5th and 95th percentiles, the bottom and top of each box represent the 25th and 75th percentiles, and the shorter and longer lines across each box represent the median and mean, respectively. The distribution at the far right (ANN) of each plot shows cumulative statistics derived from all daytime datasets during the 19-month period, and the yearly average from entire dataset is drawn across the entire plot.

Seasonal variations of cloud height and thickness in Fig. 5 are also consistent with seasonal synoptic patterns (Fig. 1). In essence, the lower cloud-base and -top heights and shallower cloud thickness during summer are associated with the persistent high pressure and dry conditions. On the other hand, the dominant low pressure systems and moist air masses during winter months result in more deep frontal clouds associated with midlatitude cyclones, which will make the MBL clouds deeper and thicker.

Figure 6 shows the probability distribution functions and cumulative distribution functions of cloud macrophysical properties for both day (solid line) and night (dashed line) from all 5-min samples during the 19-month period. As demonstrated in Fig. 6 and summarized in Table 3, the daytime and nighttime PDFs and CDFs of the MBL cloud macrophysical properties are very similar. The mean, median, and mode values of Z_{base} and Z_{top} are nearly the same throughout the year, indicating a near-normal distribution of MBL cloud-base and -top heights at the Azores. Note that ΔZ has a positive skew, whereas T_{base} and T_{top} have a negative skew. The cloud bases are nearly all below 2 km and peak at 0.8–1 km. Most cloud tops are located between 1 and 2 km, although 20% of the Z_{top} values are below 1 km and 20% are above 2 km. Because there are no significant differences in cloud-base and -top heights between day and night, the cloud thicknesses during day and night are also nearly the same with mode values of 0.2–0.4 km. Nearly 80% of the clouds are less than 1 km thick. Almost all T_{base} and T_{top} values are warmer than 270 K, indicating the MBL clouds are liquid-phase clouds in this study. Both T_{base} and T_{top} peak at 285–290 K and have tails toward a lower temperature (~270 K). The rise in lower T_{top} values at night coincides with the rise in Z_{top} to greater than 1.6 km.

b. *Microphysical properties*

Monthly means of the daytime cloud microphysical properties LWP, LWC, r_e, N_d, and optical depth (τ), as well as surface N_{CCN}, are shown in Fig. 7. Their corresponding daytime (and nighttime for LWP and LWC) PDFs and CDFs are plotted in Fig. 8 and their seasonal and yearly mean, standard deviation, median, and mode values are listed in Table 3. As demonstrated in Fig. 7a (Fig. 7b), monthly means of LWP (LWC) exceed the annual mean from April to July (for LWC from April to September), whereas averages for the other months fall below the annual mean. These results are also reflected in their seasonal means listed in Table 3 where the LWP and LWC values during spring and summer are larger than during winter and autumn. The nighttime LWP and LWC averages are about 30 g m^{-2} and 0.04 g m^{-3} larger, respectively, than their daytime values throughout the year, consistent with satellite measurements (e.g., Wood et al. 2002; O'Dell et al. 2008). Both the median and mode values in LWP and LWC are lower than their means, suggesting that there is a positive skew in LWP and LWC distributions. As illustrated in Figs. 8a and 8b, there are obviously larger LWP and LWC values at night than during the day.

Monthly mean r_e values are nearly constant and fluctuate within 1 μm around the annual mean of 12.4 μm, except for January and November when the monthly r_e means are 1.8 and 1.1 μm, respectively, below the annual

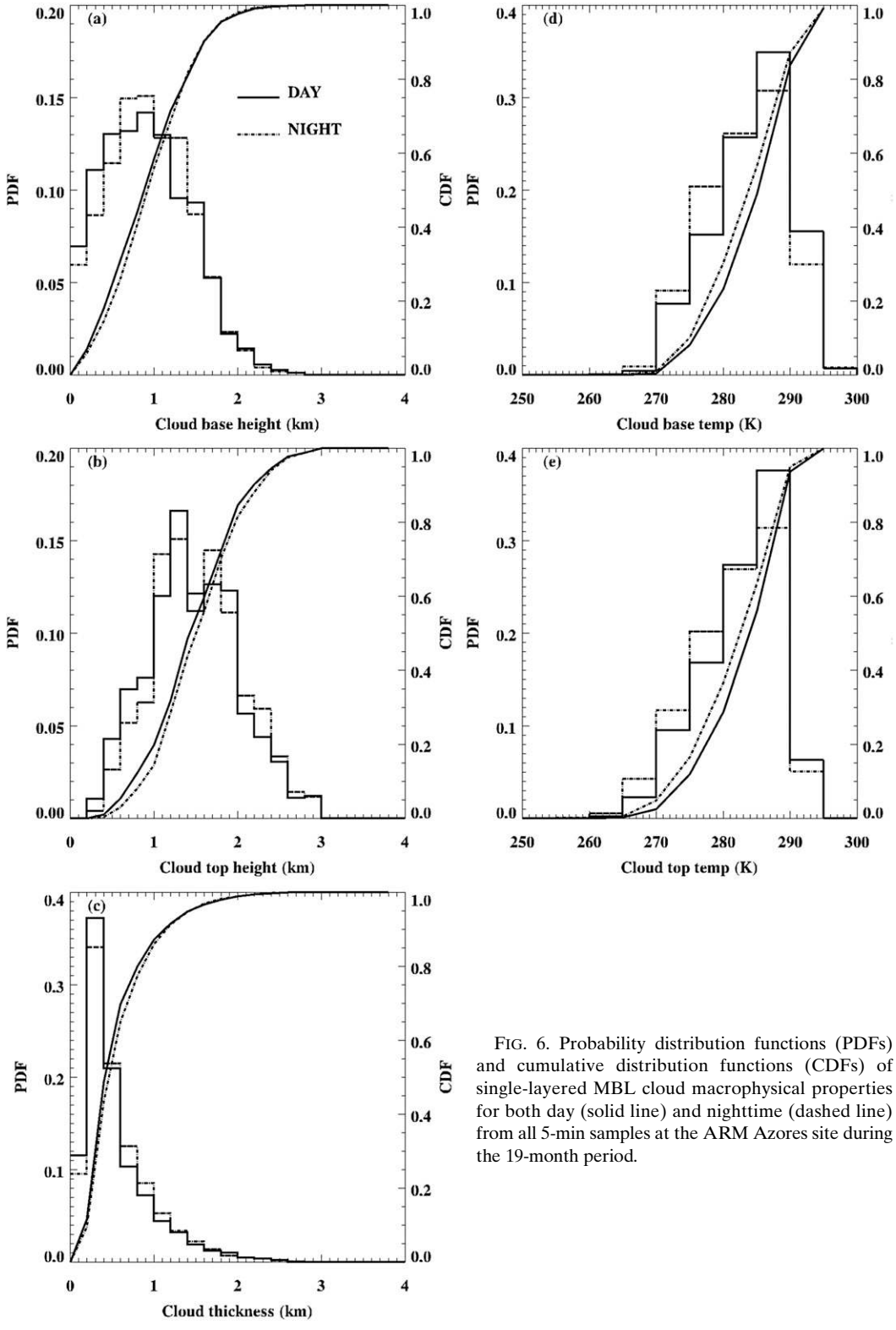

FIG. 6. Probability distribution functions (PDFs) and cumulative distribution functions (CDFs) of single-layered MBL cloud macrophysical properties for both day (solid line) and nighttime (dashed line) from all 5-min samples at the ARM Azores site during the 19-month period.

mean. These annual and monthly means represent typical MBL cloud-droplet effective radii (e.g., Dong et al. 1997; Miles et al. 2000). As listed in Table 3, the annual r_e mean, standard deviation, median, and mode are 12.5, 4.6, 11.9, and 11 μm, respectively. The PDF in Fig. 8 coupled with nearly identical mean, median, and mode r_e values indicates a near-normal distribution of r_e with a peak at 10–12 μm. Because τ was calculated from the ratio of LWP to r_e, its monthly means are nearly the same as LWP variation, given nearly constant r_e throughout the year. The annual mean of τ is 13.1 with peaks from 5 to 15.

Monthly mean N_d values fluctuate around its annual mean (82 cm^{-3}) with a long tail toward higher values as shown in Figs. 7d and 8d. Nearly 80% of the N_d values are less than 100 cm^{-3}. The method ($\sim\mathrm{LWC}/r_e^3$) to calculate N_d assumes a lognormal size distribution ($\sigma_x = 0.38$, Miles et al. 2000). With nearly constant r_e values year around, the monthly variation of N_d basically follows LWC variation (Figs. 7b–d) except during January and November because the r_e values during those two months are much smaller than the annual mean.

Monthly mean surface N_{CCN} values have a relatively large variation around the annual mean (215 cm^{-3}) with a minimum of 129 cm^{-3} during February and a maximum of 322 cm^{-3} in April. The winter (266 cm^{-3}) and spring (235 cm^{-3}) seasonal mean values are much higher than their summer (193 cm^{-3}) and autumn (196 cm^{-3}) complements. The monthly variation of N_{CCN} follows N_d variation during January–May due to the frequent low-pressure systems because upward motion can bring more surface CCN to the cloud base (well-mixed boundary layer). During summer and autumn, the correlation between N_d and N_{CCN} is not as strong as that during January–May because downward motion from high pressure systems is dominant. The correlation between N_d and N_{CCN} during the 19-month period is 0.345 with the highest correlation of 0.842 during January–June 2010 and lowest correlation of −0.93 during September–December 2009. The PDF of CCN (at 0.2% supersaturation) is similar to that of N_d with peak values ranging from 50 to 250 cm^{-3}.

Combining the daytime macrophysical properties discussed in section 4a and listed in Table 3, we can conclude that during summer the MBL cloud layer is shallow, thin, and warm with larger LWP and LWC, whereas during winter it is deep, thick, and cold with lower LWP and LWC. Note that this conclusion is totally opposite to results at the ARM SGP site (Table 2 in Dong et al. 2005) where the low cloud layers at the SGP are deeper, thicker, and warmer with less LWP and LWC during summer than during winter. These different cloud properties may be impacted by different synoptic patterns and air masses and/or physical processes/mechanisms. Therefore, a further study to investigate these differences is warranted.

c. Diurnal variation

Hourly mean single-layered MBL cloud macrophysical and microphysical properties are calculated from all available samples in each hour from the 19-month period and are illustrated in Fig. 9. Hourly mean Z_{base}, Z_{top}, and ΔZ are nearly constant with no significant day–night variation. Hourly mean cloud-base and -top temperatures fluctuate around their daily means within 1 K (Fig. 9b), with the lowest temperature during sunrise or early morning (~0600–0800 LT) and the highest temperature during late afternoon (1800 LT). These results indicate that there are no strong diurnal variations in the MBL cloud macrophysical properties at the Azores.

Strong diurnal variations, however, are seen in the cloud microphysical properties (LWP and LWC, Figs. 9c,d). There are larger nighttime LWP values (140 $\mathrm{g\,m}^{-2}$) than during the daytime (109 $\mathrm{g\,m}^{-2}$) with a semidiurnal cycle peaked at 0500 and 2100 LT, respectively. Because diurnal variation in cloud thickness is small, hourly mean LWCs are primarily determined by LWP values (Fig. 9d). Although the day − night LWC difference is small ($\mathrm{LWC}_{\mathrm{max}} - \mathrm{LWC}_{\mathrm{min}} = 0.067\ \mathrm{g\,m}^{-3}$), it is apparent that the LWC is generally greater at night than during the day. This result suggests that solar absorption at the cloud top not only suppresses the turbulence generated through nocturnal longwave radiative cooling at cloud top and MBL cloud formation, but also reduces LWC (i.e., adiabaticity).

Therefore, we can conclude that the cloud-base and -top heights, temperatures, and cloud depth are nearly invariant. There are semidiurnal cycles in both LWP and LWC with larger values at night than during the day (Figs. 9a–d). The results of this study are very similar to those derived from ship-based meteorological data during the 2008 VAMOS Ocean–Cloud–Atmosphere–Land Study Regional Experiment (VOCALS-REX) over the southeast Pacific Ocean (Burleyson et al. 2013). Figures 9e–h show daytime hourly mean r_e, N_d, N_{CCN}, and optical depth based on available retrievals. Similar to its seasonal variation, the hourly variation of r_e is also small. Hourly variation of N_d ($\sim\mathrm{LWC}/r_e^3$) basically follows LWC variation with some modification by r_e. Hourly variation of N_{CCN} is also flat with low values at sunrise and high concentrations in late afternoon. Notice that the ratios of N_d to N_{CCN} are greater during early morning and late afternoon than near local noon, probably due to more well-mixed MBLs during early morning and late afternoon and more decoupled MBLs near local noon. For cloud optical depth, the diurnal variation is similar to its seasonal variation, largely following that of LWP.

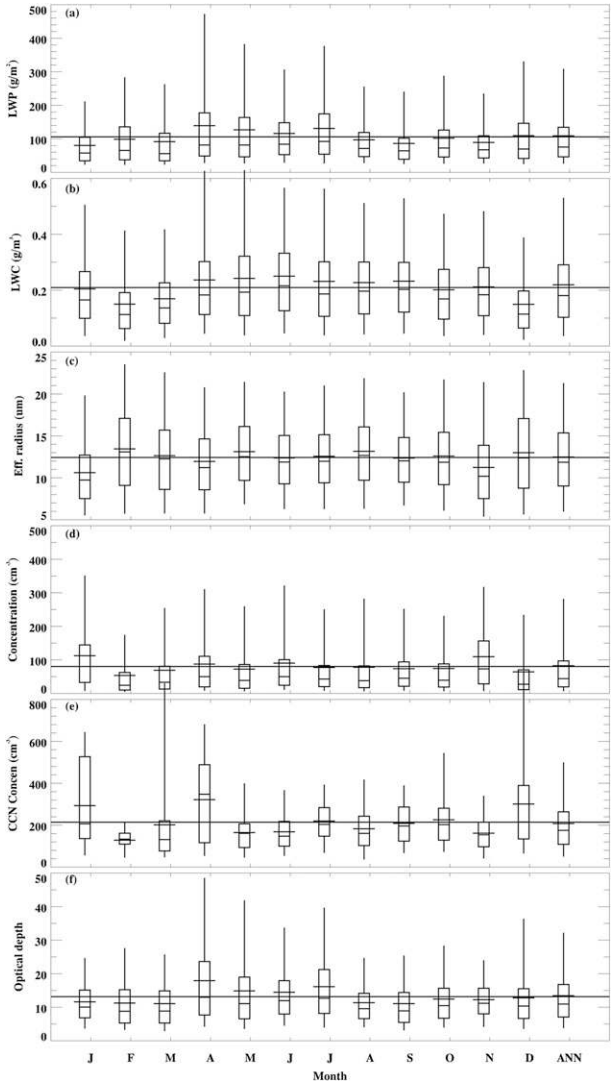

FIG. 7. As in Fig. 5, but for daytime MBL cloud microphysical properties: (a) LWP, (b) LWC, (c) cloud-droplet effective radius r_e, (d) number concentration N_d, and (f) optical depth, as well as (e) surface CCN.

d. Discussion

Table 4 summarizes the MBL cloud LWC, r_e, N_d, and N_{CCN} means retrieved from this study, and measured in situ by ASTEX aircraft during June 1992. Miles et al. (2000) generated a comprehensive database of MBL cloud microphysical properties derived from aircraft in situ measurements during various field experiments, including ASTEX, conducted before 2000. MBL cloud properties LWC, r_e, and N_d were significantly different in various field experiments in different climatic regimes, with means (standard deviations) of 0.18 g m^{-3} (0.14 g m^{-3}), 9.6 μm (2.4 μm), and 74 cm^{-3} (45 cm^{-3}). Yum and Hudson (2002) processed 17 ASTEX flights and classified them into 11 maritime and 6 continental air masses. The summarized maritime (continental) cloud microphysical properties of LWC, r_e, N_d, and N_{CCN} (0.6% supersaturation) are 0.164 g m^{-3} (0.119 g m^{-3}), 8.2 μm (6.1 μm), 86 cm^{-3} (183 cm^{-3}), and 163 cm^{-3} (1023 cm^{-3}), respectively. Those aircraft in situ measurements are consistent with the remotely sensed MBL cloud microphysical properties documented in this study although the aircraft data were all collected during a single month, June 1992. Monthly means of daytime LWC, r_e, N_d, and CCN during June are 0.25 g m^{-3}, 12.4 μm, 91 cm^{-3}, and 169 cm^{-3} in this study, and agree well with aircraft data.

Garrett and Hobbs (1995) examined two different cases: one with a clean marine air mass (12 June 1995) and a second adjacent, continentally influenced air mass (22 June 1995) near the Azores using aircraft data. Hudson and Li (1995) examined the 17 June 1995 case near the Azores using aircraft data and found two distinguishable air masses. Dong et al. (1997) found similar MBL cloud microphysical properties retrieved from ground-based measurements for the 17 June case. All of these results and the summarized maritime and continental cloud microphysical properties in Table 1 of Yum and Hudson (2002) indicate that the continentally polluted air masses can be transported to the Azores and impact MBL cloud microphysical properties. For example, polluted air masses can result in higher N_{CCN}, N_d, and smaller r_e, while the clean air masses have lower N_{CCN}, N_d, and larger r_e, but similar LWC. Different air mass sources over the Azores significantly impact cloud microphysical retrievals and surface CCN as demonstrated by the great variability in N_{CCN} and cloud microphysical properties during some months.

Note that the correlation between N_{CCN} and N_d in our study is not as strong as reported in the aircraft studies discussed above because N_{CCN} was calculated at the surface in this study while N_d was retrieved in the MBL cloud layer. Without aircraft in situ measurements, it is difficult to quantitatively answer how much of the surface CCN can be converted to N_d, and whether or not the surface CCN can represent cloud-base CCN. To validate these ground-based observations and retrievals directly, it is necessary to make comparisons between aircraft data and surface retrievals.

5. Summary and conclusions

This study is the first part of a series of papers describing the climatological MBL aerosol, cloud, and radiative properties at the ARM Azores site and documents the most comprehensive dataset of marine cloud

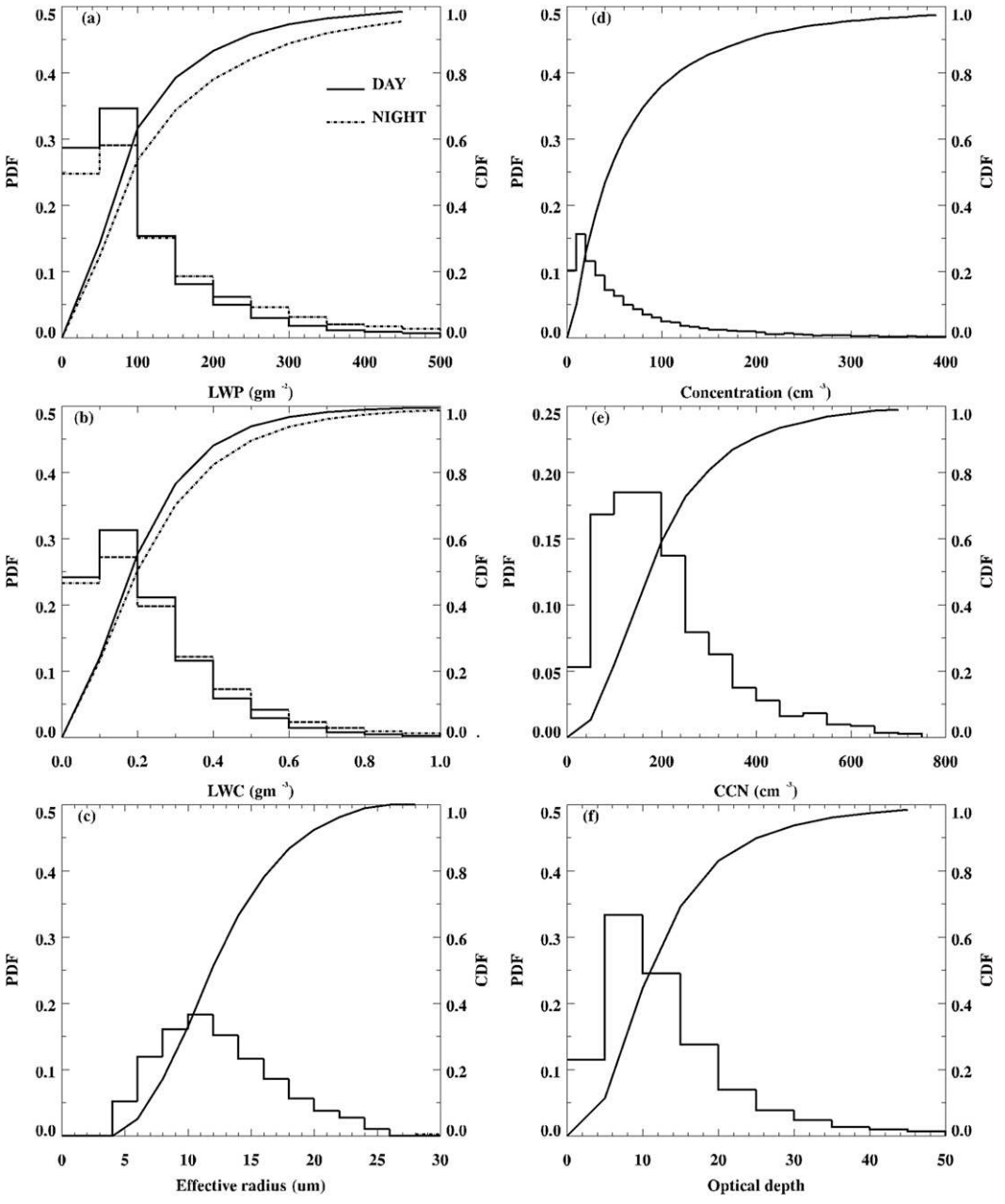

FIG. 8. As in Fig. 6, but for MBL cloud microphysical properties and surface CCN.

fraction and MBL cloud macrophysical and microphysical properties. A 19-month record of total and single-layered low (0–3 km), middle (3–6 km), and high (>6 km) cloud fractions and single-layered MBL cloud macrophysical and microphysical properties was generated from ground-based observations at the ARM Azores site between June 2009 and December 2010. This comprehensive dataset was used to examine seasonal and diurnal variations, vertical distributions as well as the impact of large-scale synoptic patterns on these MBL cloud fractions and properties. We have also compared the results in this study with other studies using aircraft in situ measurements during ASTEX. From the 19-month record of ground-based observations and retrievals, we report the following conclusions:

1) Monthly variations of total cloud fraction and single-layered low, middle, and high cloud fractions show that CF_T and CF_H were greatest during winter, while CF_L peaked during summer. Midlevel clouds occurred least frequently and were nearly invariant over the annual cycle. Both CF_T and CF_L have more

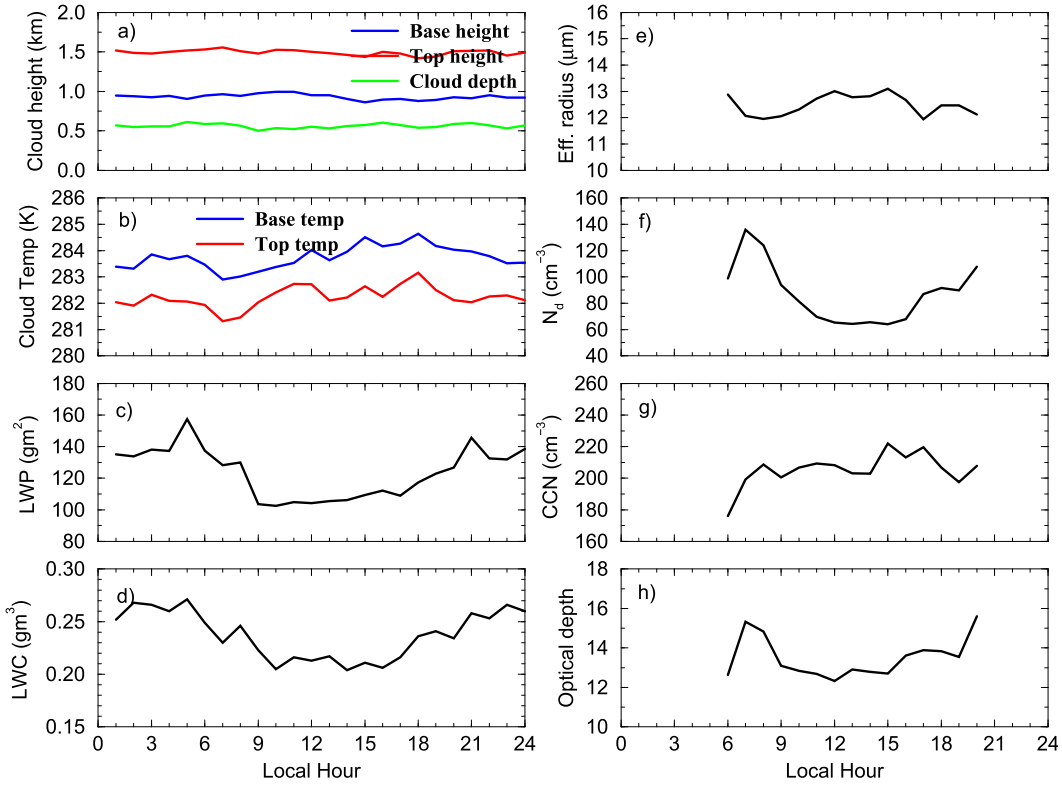

FIG. 9. As in Fig. 3, but for hourly means of single-layered MBL clouds properties from both daytime and nighttime datasets. Only daytime r_e, N_d and optical depth, and surface CCN are plotted due to available retrievals.

pronounced diurnal cycles during summer than during other seasons. The CF occurring in a given altitude band is bimodally distributed throughout the year with a lower peak at roughly 1 km and a higher peak between 8 and 11 km. During the summer, the high cloud peak is less significant than during the other seasons. There are also summer season persistent high pressure and dry weather conditions that result in more single-layered MBL clouds and less total cloudiness, whereas during winter the frequent low pressure systems and moist air masses generate more total and multilayered

TABLE 4. MBL cloud LWC, r_e, N_d, and CCN retrieved from AMF-Azores measurements in this study and measured by aircraft during ASTEX (June 1992).

Location	Air mass	LWC (g m^{-3})	r_e (μm)	N_d (cm^{-3})	CCN (cm^{-3})	Source
Azores Annual mean, daytime	Maritime with periodic pollution	0.219	12.5	82.6	207.3	This study
Azores June, daytime	Maritime with periodic pollution	0.25	12.4	90.6	168.5	This study
Azores, ASTEX	Maritime	0.164	8.2	86	163	Yum and Hudson (2002)
Azores, ASTEX	Continental	0.119	6.1	183	1023	Yum and Hudson (2002)
Different IOPs	Maritime	0.18	9.6	74		Miles et al. (2000)
Azores, ASTEX	Maritime	0.15–0.35	9.5–13.4	47		Albrecht et al. (1995)
Azores, ASTEX	Nocturnal stratus	0.01–0.37	5.8–9.8	100		Duynkerke et al. (1995)
Azores, ASTEX	Sc	0.15	10.8	50		Martin et al. (1994, 1995)
Azores, ASTEX	Maritime		9.4–13.9			Platnick and Valero (1995)
Azores, ASTEX 12 June	Maritime	0.23	7.3	174	30–100	Garrett and Hobbs (1995)
Azores, ASTEX 22 June	Continental	0.21	5.3	457	100–800	Garrett and Hobbs (1995)
Azores, ASTEX 17 June	Continental	0.2	5.4	220	668	Hudson and Li (1995)
Azores, ASTEX 17 June	Maritime	0.2	12.2	35	116	Hudson and Li (1995)
Off east coast of Australia	Maritime	0.16	11.6			Stephens and Platt (1987)

clouds, and deep frontal clouds associated with midlatitude cyclones. Because this study and Rémillard et al. (2012) complement each other, together they provide a more complete characterization of marine clouds and MBL clouds at the Azores.

2) Seasonal variations of cloud heights and thickness are strongly associated with seasonal synoptic patterns. For example, lower cloud-base and -top heights and diminished cloud thickness during summer are associated with persistent high pressure and dry conditions. In contrast, predominant low pressure systems and moist air masses during winter result in more deep frontal clouds associated with midlatitude cyclones, which make the MBL cloud layer deeper and thicker. Therefore, in terms of LWP and LWC, during the summer the MBL cloud layer is shallow, thin, and warm with larger LWP and LWC, whereas during winter it is deep, thick, and cold with lower LWP and LWC. Cloud-base and -top heights and temperatures and cloud depth are nearly invariant diurnally. There are also semidiurnal cycles in both LWP and LWC with larger values at night than during the day.
3) Monthly daytime r_e means are nearly constant and fluctuate within 1 μm of the annual mean of 12.4 μm. Monthly variation of N_d basically follows the LWC variation. There is a strong correlation between N_{CCN} and N_d during January–May owing to the frequent low pressure systems. During summer and autumn, the correlation between N_d and N_{CCN} is not as strong as during January–May when downward motion from high pressure systems is dominant. Although taken during different periods, the cloud microphysical retrievals in this study agree with ASTEX aircraft data. Various air mass sources over the Azores significantly impact the cloud microphysical retrievals and surface CCN as demonstrated by the great variability in N_{CCN} calculations and cloud microphysical properties during some months.

These results can serve as a baseline for studying MBL cloud fractions, and macrophysical and microphysical properties. These results can also serve as ground truth for validating satellite-retrieved MBL cloud properties at the Azores (Xi et al. 2013, manuscript submitted to *J. Geophys. Res. Atmos.*). This 19-month dataset over the ARM Azores site should also provide statistically reliable estimates of monthly and diurnal variations of cloud fractions and properties for climate and numerical modelers to verify their simulated MBL cloud fractions and properties. The conclusions reached here are based only on ground-based observations, and a further validation study using coincident aircraft in situ measurements is required. Future installments of this series will report on the impact of clouds on surface and TOA radiation budgets as well as MBL aerosol–cloud interactions at the Azores.

Acknowledgments. The data were obtained from the Atmospheric Radiation Measurement (ARM) Program sponsored by the U.S. Department of Energy (DOE) Office of Energy Research, Office of Health and Environmental Research, Environmental Sciences Division. This study was primarily supported by the NASA CERES project at the University of North Dakota project under Grant NNX10AI05G and by the DOE ASR project at the University of North Dakota under a grant with Award DE-SC0008468. Dr. Robert Wood was supported by the DOE ASR project at the University of Washington with Award DE-SC0006865MOD0002. Patrick Minnis was supported by the DOE ASR program under Interagency Grant DE-SC0000991/003. Special thanks to Dr. Long, who provided the clear-sky SW fluxes over the ARM Azores site.

REFERENCES

Albrecht, B. A., C. S. Bretherton, D. Johnson, W. H. Scubert, and A. S. Frisch, 1995: The Atlantic Stratocumulus Transition Experiment—ASTEX. *Bull. Amer. Meteor. Soc.,* **76,** 889–904, doi:10.1175/1520-0477(1995)076<0889:TASTE>2.0.CO;2.

Bony, S., and J.-L. Dufresne, 2005: Marine boundary layer clouds at the heart of tropical cloud feedback uncertainties in climate models. *Geophys. Res. Lett.,* **32,** L20806, doi:10.1029/2005GL023851.

Burleyson, C. D., S. P. de Szoeke, S. E. Yuter, M. Wilbanks, and W. A. Brewer, 2013: Ship-based observations of the diurnal cycle of southeast Pacific marine stratocumulus clouds and precipitation. *J. Atmos. Sci.,* **70,** 3876–3894, doi:10.1175/JAS-D-13-01.1.

Cess, R. D., and Coauthors, 1990: Intercomparison and interpretation of climate feedback processes in 19 atmospheric general circulation models. *J. Geophys. Res.,* **95,** 16 601–16 615, doi:10.1029/JD095iD10p16601.

——, and Coauthors, 1996: Cloud feedback in atmospheric general circulation models: An update. *J. Geophys. Res.,* **101,** 12 791–12 794, doi:10.1029/96JD00822.

Clothiaux, E. E., T. P. Ackerman, G. G. Mace, K. P. Moran, R. T. Marchand, M. A. Miller, and B. E. Martner, 2000: Objective determination of cloud heights and radar reflectivities using a combination of active remote sensors at the ARM CART sites. *J. Appl. Meteor.,* **39,** 645–665, doi:10.1175/1520-0450(2000)039<0645:ODOCHA>2.0.CO;2.

Dolinar, E., X. Dong, B. Xi, A. Kennedy, J. Jiang, P. Minnis, and H. Su, 2014: Evaluation of CMIP GCMs simulated cloud fraction and TOA radiation budgets using NASA satellite observations. *Climate Dyn.,* in press.

Dong, X., and G. G. Mace, 2003: Profiles of low-level stratus cloud microphysics deduced from ground-based measurements. *J. Atmos. Oceanic Technol.,* **20,** 42–53, doi:10.1175/1520-0426(2003)020<0042:POLLSC>2.0.CO;2..

——, T. P. Ackerman, E. E. Clothiaux, P. Pilewskie, and Y. Han, 1997: Microphysical and radiative properties of stratiform

clouds deduced from ground-based measurements. *J. Geophys. Res.,* **102,** 23 829–23 843, doi:10.1029/97JD02119.

——, ——, and ——, 1998: Parameterizations of microphysical and shortwave radiative properties of boundary layer stratus from ground-based measurements. *J. Geophys. Res.,* **103,** 31 681–31 393, doi:10.1029/1998JD200047.

——, P. Minnis, T. P. Ackerman, E. E. Clothiaux, G. G. Mace, C. N. Long, and J. C. Liljegren, 2000: A 25-month database of stratus cloud properties generated from ground-based measurements at the ARM SGP site. *J. Geophys. Res.,* **105,** 4529–4537, doi:10.1029/1999JD901159.

——, ——, G. G. Mace, W. L. Smith Jr., M. Poellot, R. Marchand, and A. Rapp, 2002: Comparison of stratus cloud properties deduced from surface, GOES, and aircraft data during the March 2000 ARM Cloud IOP. *J. Atmos. Sci.,* **59,** 3265–3284, doi:10.1175/1520-0469(2002)059<3265:COSCPD>2.0.CO;2.

——, ——, and B. Xi, 2005: A climatology of midlatitude continental clouds from the ARM SGP Central Facility: Part I: Low-level cloud macrophysical, microphysical and radiative properties. *J. Climate,* **18,** 1391–1410, doi:10.1175/JCLI3342.1.

Duynkerke, P. G., H. Zhang, and P. T. Jonker, 1995: Microphysical and turbulent structure of nocturnal stratocumulus as observed during ASTEX. *J. Atmos. Sci.,* **52,** 2763–2777, doi:10.1175/1520-0469(1995)052<2763:MATSON>2.0.CO;2.

Garrett, T. J., and P. V. Hobbs, 1995: Long-range transport of continental aerosols over the Atlantic Ocean and their effects on cloud structures. *J. Atmos. Sci.,* **52,** 2977–2984, doi:10.1175/1520-0469(1995)052<2977:LRTOCA>2.0.CO;2.

Hartmann, D. L., and D. Short, 1980: On the use of earth radiation budget statistics for studies of clouds and climate. *J. Atmos. Sci.,* **37,** 1233–1250, doi:10.1175/1520-0469(1980)037<1233:OTUOER>2.0.CO;2.

Houghton, J. T., and Coauthors, Eds., 2001: *Climate Change 2001: The Scientific Basis*. Cambridge University Press, 881 pp.

Hudson, J. G., and H. Li, 1995: Microphysical contrasts in Atlantic stratus. *J. Atmos. Sci.,* **52,** 3031–3040, doi:10.1175/1520-0469(1995)052<3031:MCIAS>2.0.CO;2.

——, and S. Noble, 2014: CCN and vertical velocity influences on droplet concentrations and supersaturations in clean and polluted stratus clouds. *J. Atmos. Sci.,* **71,** 312–331.

Jefferson, A., 2010: Empirical estimates of CCN from aerosol optical properties at four remote sites. *Atmos. Chem. Phys.,* **10,** 6855–6861, doi:10.5194/acp-10-6855-2010.

Jiang, J., and Coauthors, 2012: Evaluation of cloud and water vapor simulations in CMIP5 climate models using NASA ''A-train'' satellite observations. *J. Geophys. Res.,* **117,** D14105, doi:10.1029/2011JD017237.

Klein, S. A., and D. L. Hartmann, 1993: The seasonal cycle of stratiform clouds. *J. Climate,* **6,** 1587–1606, doi:10.1175/1520-0442(1993)006<1587:TSCOLS>2.0.CO;2.

——, Y. Zhang, M. D. Zelinka, R. Pincus, J. Boyle, and P. J. Gleckler, 2013: Are climate model simulations of clouds improving? An evaluation using the ISCCP simulator. *J. Geophys. Res.,* **118,** 1329–1342, doi:10.1002/jgrd.50141.

Liljegren, J. C., E. E. Clothiaux, G. G. Mace, S. Kato, and X. Dong, 2001: A new retrieval for cloud liquid water path using a ground-based microwave radiometer and measurements of cloud temperature. *J. Geophys. Res.,* **106,** 14 485–14 500, doi:10.1029/2000JD900817.

Lilly, D. K., 1968: Models of cloud-topped mixed layers under a strong inversion. *Quart. J. Roy. Meteor. Soc.,* **94,** 292–309, doi:10.1002/qj.49709440106.

Lin, W., M. Zhang, and N. G. Loeb, 2009: Seasonal variation of the physical properties of marine boundary layer clouds off the California coast. *J. Climate,* **22,** 2624–2638, doi:10.1175/2008JCLI2478.1.

Logan, T., B. Xi, and X. Dong, 2014: Aerosol physical and chemical properties and their interaction with CCN over the AMF-Azores facility. *J. Geophys. Res. Atmos.,* in press.

Long, C. N., and Y. Shi, 2008: An automated quality assessment and control algorithm for surface radiation measurements. *Open Atmos. Sci. J.,* **2,** 23–37, doi:10.2174/1874282300802010023.

Martin, G. M., D. W. Johnson, and A. Spice, 1994: The measurement and parameterization of effective radius of drops in warm stratocumulus clouds. *J. Atmos. Sci.,* **51,** 1823–1842, doi:10.1175/1520-0469(1994)051<1823:TMAPOE>2.0.CO;2.

——, D. P. Rogers, P. R. Jonas, P. Minnis, and D. A. Hegg, 1995: Observations of the interaction between cumulus clouds and warm stratocumulus clouds in the marine boundary layer during ASTEX. *J. Atmos. Sci.,* **52,** 2902–2922, doi:10.1175/1520-0469(1995)052<2902:OOTIBC>2.0.CO;2.

Mather, J. H., and J. W. Voyles, 2013: The ARM Climate Research Facility: A review of structure and capabilities. *Bull. Amer. Meteor. Soc.,* **94,** 377–392, doi:10.1175/BAMS-D-11-00218.1.

Mead, J. B., and K. B. Widener, 2005: W-band ARM cloud radar. Preprints, *32nd Int. Conf. on Radar Meteorology,* Albuquerque, NM, Amer. Meteor. Soc., P1R.3. [Available online at http://ams.confex.com/ams/pdfpapers/95978.pdf.]

Miles, N. L., J. Verlinde, and E. E. Clothiaux, 2000: Cloud-droplet size distributions in low-level stratiform clouds. *J. Atmos. Sci.,* **57,** 295–311, doi:10.1175/1520-0469(2000)057<0295:CDSDIL>2.0.CO;2.

O'Dell, C. W., F. J. Wentz, and R. Bennartz, 2008: Cloud liquid water path from satellite-based passive microwave observations: A new climatology over the global oceans. *J. Climate,* **21,** 1721–1739, doi:10.1175/2007JCLI1958.1.

Paluch, J. R., and D. H. Lenschow, 1991: Stratiform cloud formation in the marine boundary layer. *J. Atmos. Sci.,* **48,** 2141–2158, doi:10.1175/1520-0469(1991)048<2141:SCFITM>2.0.CO;2.

Platnick, S., and F. P. J. Valero, 1995: A validation of a satellite cloud retrieval during ASTEX. *J. Atmos. Sci.,* **52,** 2985–3001, doi:10.1175/1520-0469(1995)052<2985:AVOASC>2.0.CO;2.

Rémillard, J., P. Kollias, E. Luke, and R. Wood, 2012: Marine boundary layer cloud observations in the Azores. *J. Climate,* **25,** 7381–7398, doi:10.1175/JCLI-D-11-00610.1.

Rossow, W. B., and R. A. Schiffer, 1991: International Satellite Cloud Climatology Project (ISCCP) cloud data products. *Bull. Amer. Meteor. Soc.,* **72,** 2–20, doi:10.1175/1520-0477(1991)072<0002:ICDP>2.0.CO;2.

Slingo, A., 1990: Sensitivity of the earth's radiation budget to changes in low clouds. *Nature,* **343,** 49–51, doi:10.1038/343049a0.

Soden, B. J., and G. A. Vecchi, 2011: The vertical distribution of cloud feedback in coupled ocean–atmosphere models. *Geophys. Res. Lett.,* **38,** L12704, doi:10.1029/2011GL047632.

Stanfield, R., X. Dong, B. Xi, A. Del Genio, P. Minnis, and J. Jiang, 2014: Assessment of NASA GISS CMIP5 and post-CMIP5 simulated clouds and TOA radiation budgets using satellite observations: Part I: Cloud fraction and microphysical properties. *J. Climate,* doi:10.1175/JCLI-D-13-00558.1, in press.

Stephens, G. L., and C. M. R. Platt, 1987: Aircraft observations of the radiative and microphysical properties of stratocumulus and cumulus cloud fields. *J. Climate Appl. Meteor.,* **26,** 1243–1269, doi:10.1175/1520-0450(1987)026<1243:AOOTRA>2.0.CO;2.

Taylor, K. E., R. J. Stouffer, and G. A. Meehl, 2012: An overview of CMIP5 and the experiment design. *Bull. Amer. Meteor. Soc.,* **93,** 485–498, doi:10.1175/BAMS-D-11-00094.1.

Wielicki, B. A., R. D. Cess, M. D. King, D. A. Randall, and E. F. Harrison, 1995: Mission to planet Earth: Role of clouds and radiation in climate. *Bull. Amer. Meteor. Soc.,* **76,** 2125–2153, doi:10.1175/1520-0477(1995)076<2125:MTPERO>2.0.CO;2.

Wood, R., 2009: Clouds, Aerosol, and Precipitation in the Marine Boundary Layer (CAP-MBL). DOE/SC-ARM-0902, 23 pp. [Available online at http://www.arm.gov/publications/programdocs/doe-sc-arm-0902.pdf?id=94.]

——, 2012: Review: Stratocumulus clouds. *Mon. Wea. Rev.,* **140,** 2373–2423, doi:10.1175/MWR-D-11-00121.1.

——, C. S. Bretherton, and D. L. Hartmann, 2002: Diurnal cycle of liquid water path over the subtropical and tropical oceans. *Geophys. Res. Lett.,* **29,** 2092, doi:10.1029/2002GL015371.

Xi, B., X. Dong, P. Minnis, and M. M. Khaiyer, 2010: A 10-year climatology of cloud cover and vertical distribution derived from both surface and GOES observations over the DOE ARM SGP Site. *J. Geophys. Res.,* **115,** D12124, doi:10.1029/2009JD012800.

Yoo, H., and Z. Li, 2012: Evaluation of cloud properties in the NOAA/NCEP Global Forecast System using multiple satellite products. *Climate Dyn.,* **39,** 2769–2787, doi:10.1007/s00382-012-1430-0.

——, ——, Y.-T. Hou, S. Lord, F. Weng, and H. W. Barker, 2013: Diagnosis and testing of low-level cloud parameterizations for the NCEP/GFS using satellite and ground-based measurements. *Climate Dyn.,* **41,** 1595–1613, doi:10.1007/s00382-013-1884-8.

Yum, S. S., and J. G. Hudson, 2002: Maritime/continental microphysical contrasts in stratus. *Tellus,* **54B,** 61–73, doi:10.1034/j.1600-0889.2002.00268.x.